Journal of Applied Remote Sensing

RemoteSensing.SPIEDigitalLibrary.org

Development of aboveground mangrove forests' biomass dataset for Southeast Asia based on ALOS-PALSAR 25-m mosaic

Soni Darmawan
Dewi K. Sari
Wataru Takeuchi
Ketut Wikantika
Rika Hernawati

SPIE.

Soni Darmawan, Dewi K. Sari, Wataru Takeuchi, Ketut Wikantika, Rika Hernawati, "Development of aboveground mangrove forests' biomass dataset for Southeast Asia based on ALOS-PALSAR 25-m mosaic," *J. Appl. Remote Sens.* **13**(4), 044519 (2019), doi: 10.1117/1.JRS.13.044519.

Development of aboveground mangrove forests' biomass dataset for Southeast Asia based on ALOS-PALSAR 25-m mosaic

Soni Darmawan,[a,*] Dewi K. Sari,[a] Wataru Takeuchi,[b] Ketut Wikantika,[c] and Rika Hernawati[a]

[a]Institut Teknologi Nasional Bandung, Department of Geodetic Engineering, Bandung, Indonesia

[b]University of Tokyo, Institute of Industrial Science, Tokyo, Japan

[c]InstitutTeknologi Bandung, Center for Remote Sensing, Bandung, Indonesia

Abstract. Southeast Asia (SEA) has the largest mangrove forest area in the world, which plays an important role in the global carbon cycle and is helping to mitigate climate change. In order to manage the mangrove forests in SEA, their total biomass needs to be determined. However, development of a biomass dataset based on field survey is time consuming. An aboveground biomass (AGB) dataset of mangrove forests was developed for SEA based on ALOS PALSAR 25-m mosaic. Specifically, ALOS-PALSAR 25-m images were first retrieved for SEA from the Kyoto and Carbon Initiative projects and then converted from a digital number to a normalized radar cross-section format in decibels. Samples of mangrove forests in SEA were collected as regions of interest from ALOS PALSAR data based on visual interpretation using Landsat data and Google Earth imagery. A rule-based classification method based on mangrove backscattering characteristics was then used to classify mangroves and nonmangroves in the region. Subsequently, an empirical model was adopted to estimate the AGB of the mangrove forests and an AGB dataset was developed. The results indicate that the spatial distribution of mangrove forests over SEA is 5.1 million hectares, and the estimated average AGB is 140.5 ± 136.1 Mg/ha. [DOI: 10.1117/1.JRS.13.044519]

Keywords: aboveground biomass; mangrove forests; Southeast Asia; ALOS PALSAR; backscattering.

Paper 190250 received Apr. 25, 2019; accepted for publication Nov. 1, 2019; published online Nov. 22, 2019.

1 Introduction

Mangroves are a unique and complex major component of coastal zones in the tropics and subtropics. They represent the transitional ecosystem at the confluence of sea, land, and fresh water. The main components of their vegetation are generally evergreen trees or shrubs that grow along the coastlines, estuaries, brackish water, or deltas.[1] Mangroves provide important products and various ecosystem services.[2] They not only play an important role in the sustainability of coastal ecosystems but also provide important socioeconomic and cultural benefits for coastal communities.[1] They are also known as the most intense coastal carbon absorbers in the world and play a central and growing role in the global carbon cycle.[3] According to Donato et al.,[4] the amount of carbon storage per unit area of mangrove forests is five times larger than that estimated for temperate, boreal, and tropical terrestrial forests. The high growth rates of trees and plants, anaerobic soils, and stagnant water that can retard decomposition of biomass enable mangrove forests to store a large amount of carbon over the long term.[5]

According to Alongi and Dixon,[6] mangroves are very productive ecosystems that have primary production levels equivalent to moist tropical forests and coral reefs. Mangroves only

*Address all correspondence to Soni Darmawan, E-mail: soni_darmawan@itenas.ac.id

occupy 0.5% of the global coastal area, but they contribute 10% to 15% (24 Tg C y^{-1}) of coastal sediment carbon storage and export 10% to 11% of particulate terrestrial carbon to the sea. Currently, their contribution to carbon sequestration is one of the important ways for conservation and restoration, and it further helps to reduce the greenhouse effect. This shows that mangroves play an important role in global climate change mitigation. In order to acquire and build strong awareness of global carbon conditions and the impacts of diminishing mangrove forests on climate change, it is very important to assess and quantify the spatial distribution of mangrove forests and carbon stocks, as well as the emission factors of greenhouse gases emitted from the major land use activities in mangrove forests. However, most countries, especially in Southeast Asia (SEA), do not have enough information about the total quantity of their mangrove biomass.[5,7]

From a global perspective, SEA has the largest mangrove area in the world estimated at more than 6.8 million hectares or around 34% to 42% of the total area of mangrove forests in the world.[2] Mangrove forests in SEA are the most diverse in the world[8] but have been suffering from human interference in destructive ways due to conversion of mangrove areas for agriculture, tourism, and housing.[9] According to Giri et al.,[10] the world's mangrove forests are currently estimated to have been reduced by 50% from their previous state and, estimating by their current reduction rate, 30% to 40% of coastal wetlands and 100% of mangrove forests could be lost in the next 100 years if there is no improved management to conserve them. It is strongly recommended that mangrove biomass be mapped and monitored immediately. However, conducting field surveys for mangrove biomass and its productivity in the area has proved to be very difficult as it is expensive and time consuming by nature, caused by muddy soil conditions, the weight of wood,[11,12] the vast area to cover, and tidal influences.

Remote sensing has been widely proven to be a fast, cost-effective, and efficient method for monitoring and mapping the highly spatial distribution and biomass of mangrove forests as well as their disturbance on regional and global scales.[12,13] Optical imagery and synthetic aperture radar (SAR) data have the potential to predict the biomass of tropical forests.[14] However, according to Häme et al.,[14] the depth and thickness of the irregular atmospheric conditions in the area of interest make atmospheric correction of optical images difficult. On the other hand, radiometric correction of the topography of SAR data will require a very accurate digital elevation model unless the study location is relatively flat. In particular, in tropical areas with prevalent cloud cover, SAR data are better than optical data for multitemporal acquisition.

According to Henderson and Lewis,[15] although sensors in the optical range of the electromagnetic spectrum have received the greatest attention and have been widely used, considerable effort has also been invested in the use of radar sensors. Backscatter radar is very sensitive to the dielectric properties (soil moisture and vegetation) and attributes of the geometric conditions (surface roughness) of objects on the surface of Earth.[16] In many regions of the world (e.g., areas covered by clouds and/or lacking light), radar is the only sensor that can provide consistent and periodic data in a reliable manner. A radar sensor can obtain information in the electromagnetic spectrum of the bands K, X, C, L, and P (different wavelengths) with polarizations of Horizontal to Horizontal (HH), Vertical to Vertical (VV), Horizontal to Vertical (HV), or Vertical to Horizontal (VH), which have varying ranges and azimuth resolutions. Each of these wavelengths has unique characteristics related to reflection from forest stands. The X band interacts only with leaves and canopy cover surfaces; hence, it is very suited for information on the surface layer of the tree canopy. The C band can penetrate through the leaves and spread to small branches and other underlying objects. The L band, which has a higher penetration capability, can penetrate the surface layer and spread to the stems and main branches.[17] The P band has the greatest penetration capability and can penetrate into the canopy covers. Therefore, backscatters from the L and P bands are the parameters most associated with the biophysical parameters of trees and are predominantly used for studies related to forest biomass.[18] Long-wavelength radar sensors such as L and P bands have both the advantage of being very sensitive to forest biomass and the potential for observation with high spatial and temporal resolution for estimating and monitoring biomass.[19–21]

The launch of the Japanese Space Exploration Agency's (JAXA) Advanced Land Observing Satellite (ALOS) Phased Arrayed L-band SAR (PALSAR) in 2006, therefore, represented a milestone in the global observation, characterization, mapping, and monitoring of mangroves

over a larger area. ALOS PALSAR has been proven to have the potential to estimate the aboveground biomass (AGB) of mangrove forests.[11,22,23–26] Many researchers have tried to identify the baseline mangrove forest in regional-global areas.[27–29] However, references for estimating the biomass of mangrove forests in regional-global areas are lacking, which is both a challenge and an opportunity.[30] This study was conducted with the objective of developing an aboveground mangrove forests biomass dataset for SEA based on the ALOS PALSAR 25-m mosaic.

2 Methodology

The methodology used in this study consisted of several steps. First, the study area was circumscribed and primary and secondary data were collected. Primary data were taken from ALOS PALSAR, and secondary data were obtained from land cover maps, Landsat image data, and high-resolution image data obtained from Google Earth. Data processing involved conversion of digital numbers (DN) to normalization of radar cross sections (NRCS). Training samples of the mangrove forests in the study area were delineated, backscattering characterization was performed by calculating the mean and standard deviation, mangrove forests were classified based on backscattering characterization, and the AGB of mangrove forests in SEA was estimated based on an empirical model.

2.1 *Study Site*

According to Giesen et al.,[2] the mangrove forests in SEA spread from the Irrawaddy delta in northwest Myanmar throughout the coasts of Thailand, Cambodia, and Vietnam, and over the archipelagos of the Philippine and Indonesian Archipelago from Papua island to Sumatra island. They cover more than 17,000 islands and stretch more than 6000 km from the east to the west and about 3500 km from the north to the south of SEA. The most extensive mangrove areas in SEA are found in Indonesia, followed by Malaysia and Myanmar. In this study, we collected regions of interest (ROIs) of mangrove forests on 46 sites that spread over SEA as presented in Fig. 1 and Table 1.

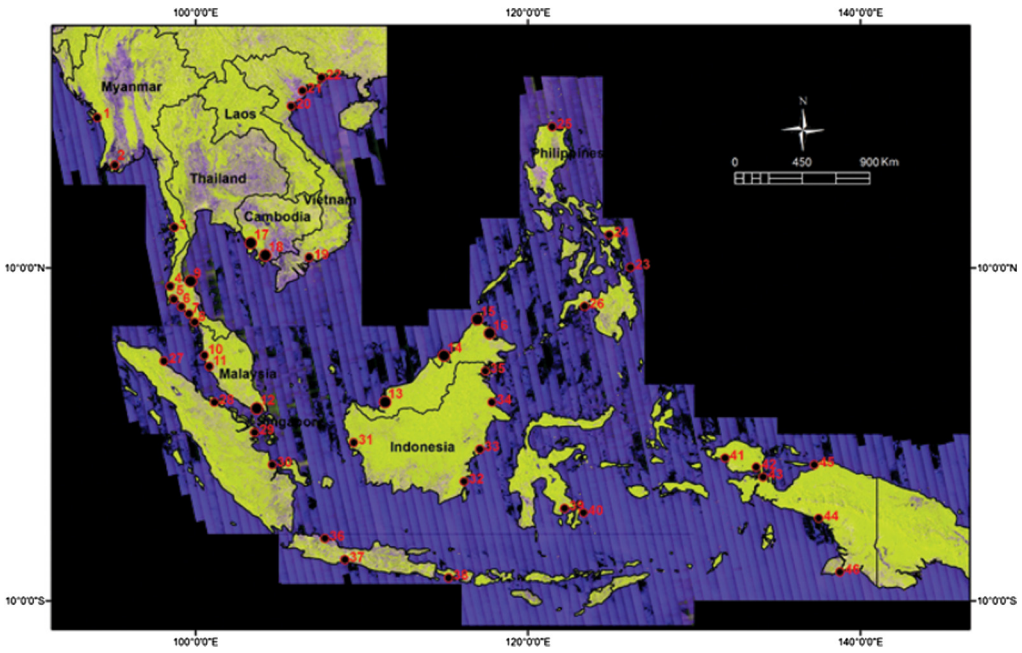

Fig. 1 Study sites based on ALOS PALSAR composite and distribution of 46 sites for collecting ROIs of mangrove forest.

Table 1 ROIs on 46 sites of mangrove forest.

No	Country/area	Coordinate	ROIs (pixels)
Myanmar			
1.	Lay Taung	19°16′N 93°58′E	8.027
2.	Meinmahla Kyun-Irrawaddy delta	15°51′N 64°56′E	3.860
3.	Tanintttharyi National Park	11°53′N 98°42′E	46.268
Thailand			
4.	Shi Phang Nga National Park	08°58′N 98°22′E	2.112
5.	Phang Nga Ko Sriboya Krabi	08°23′N 98°31′E	6.339
6.	Khlong Krabi	07°54′N 99°04′E	1.774
7.	Suso Palian Trang	07°11′N 99°39′E	7.968
8.	Puyu Mueng Satun	06°40′N 99°56′E	4.833
9.	Pak Phanang Fangtawanok	08°25′N 100°10′E	5.217
Malaysia			
10.	Jebong Matang Perak	04°49′N 100°36′E	14.579
11.	Pulau Kelang Selangor	02°59′N 101°18′E	7.923
12.	Serkat Johor	01°23′N 103°30′E	3.303
13.	Sarikei Sarawak	02°07′N 111°23′E	18.143
14.	Pulau Selirong, Brunei	04°50′N 115°07′E	5.120
15.	Kota Marudu Sabah	06°33′N 116°46′E	1.200
16.	Beluran Sabah	06°14′N 117°36′E	11.049
Cambodia			
17.	Peam Krasaop Wildlife Sanctuary	11°28′N 103°01′E	3.166
18.	Preak Piphot River	10°40′N 103°52′E	1.275
Vietnam			
19.	Thạnh An Cần Giò	10°33′N 106°52′E	13.967
20.	Giao Thiện Giao Thuỷ Nam Định	20°13′N 106°31′E	390
21.	Thái Thủy Thai Binh	20°34′N 106°36′E	730
22.	Móng Cái Quảng Ninh	21°27′N 107°55′E	881
Philippines			
23.	Siargao island	09°55′N 125°58′E	1.108
24.	Santa Margarita Samar	18°21′N 121°35′E	541
25.	Abulug Cagayan	18°21′N 121°35′E	970
26.	Dinas Zamboanga del Sur	07°34′N 123°22′E	716
Indonesia			
27.	Langsa Aceh	04°31′N 98°01′E	10.199
28.	Bengkalis Riau	02°01′N 101°36′E	14.516

Table 1 (*Continued*).

No	Country/area	Coordinate	ROIs (pixels)
29.	Indragiri Hilir Riau	00°02′S 103°29′E	40.262
30.	Banyuasin South Sumatera	01°58′S 104°32′E	74.398
31.	Pontianak West Kalimantan	00°39′S 109°28′E	36.615
32.	Kotabaru South Kalimantan	02°55′S 116°05′E	25.237
33.	Kutai Kartanegara East Kalimantan	01°02′S 116°42′E	16.728
34.	Berau East Kalimantan	02°04′N 117°39′E	33.413
35.	Nunukan East Kalimatan	04°08′N 117°20′E	33.699
36.	Subang West Java	06°13′S 107°45′E	25
37.	Cilacap Central Java	07°41′S 108°54′E	9.437
38.	Badung Bali	08°43′S 115°11′E	1.275
39.	Bombana Southeast Sulawesi	04°31′S 122°5′E	7.975
40.	Muna Southeast Sulawesi	04°44′S 123°4′E	14.111
41.	Sorong West Papua	01°21′S 131°34′E	38.666
42.	Teluk Bintuni Papua	02°9′S 133°36′E	95.396
43.	Teluk Bintuni Papua	02°34′S 133°47′E	118.867
44.	Waropen Papua	05°06′S 137°31′E	256.657
45.	Asmat Papua	01°48′S 137°21′E	91.473
46.	Merauke Papua	08°15′S 138°54′E	34.947

2.2 *Data Collection*

We used 25-m resolution PALSAR mosaic data generated by applying a high JAXA processing and analysis technique to images obtained from the Japanese L-band Synthetic Aperture Radars (PALSAR and PALSAR-2). Global 25-m resolution PALSAR/PALSAR-2 mosaic is a global SAR image made by SAR image mosaics of the backscattering coefficient measured by PALSAR/PALSAR-2. ALOS PALSAR data have been collected as part of the Kyoto and Carbon Initiative projects. As a result, we obtained a total of 60 ALOS PALSAR mosaic tiles for the SEA region. For secondary data to support the collection of training samples of mangrove areas, we used land cover maps from each country and Landsat data as well as high-resolution image data from Google Earth.

2.3 *Preprocessing*

The preprocessing focused on converting the HH (Digital Number on Horizontal to Horizontal) and HV (Digital Number on Horizontal to Vertical) values to NRCS in decibels (dB) (i.e., σ° HH and σ° HV) using the following equations:[31]

$$\sigma^\circ\mathrm{HH} = 10\log_{10}(\mathrm{DN}^2) - \mathrm{CF}, \tag{1}$$

$$\sigma^\circ\mathrm{HV} = 10\log_{10}(\mathrm{DN}^2) - \mathrm{CF}, \tag{2}$$

where σ° is the backscattering coefficient and CF is the calibration factor. CF is equal to -83 for both HH and HV.

2.4 *Characterization*

We collected mangrove samples data for the ROIs throughout the SEA region on ALOS PALSAR data based on visual interpretation using Landsat data and Google Earth images. As many as 46 ROIs of mangrove forests scattered in the SEA region were collected. The size of each ROI differed for each area of mangroves, as it depends on the size of the mangrove area in each region. After the ROI samples were obtained and the mean and standard deviation of the backscatter value for each sample were calculated. The equations for the mean and standard deviation are as follows:

$$\mu_X = \overline{X} = \frac{1}{n}\sum_{i=1}^{n} X_i, \tag{3}$$

$$\sigma = \sqrt{\frac{1}{n}\sum_{i=1}^{n}(X_i - \overline{X})^2}, \tag{4}$$

where n is the number of samples taken, X_i is the value of the sample, and $\overline{X}$ is the average of the samples.

2.5 *Classification*

The classification of mangrove forests was performed based on the characteristics of the mangrove backscatter in each training sample. We used a rule-based classification method based on the mangrove backscattering characteristics to classify mangrove and nonmangrove areas in the region. The main parameters used in this rule-based classification were the mean and standard deviation of the backscatter value image of ALOS PALSAR. All pixels in the mangrove areas were identified using the following rule-based classification algorithm:[12]

$$\text{If } \mu\_i\text{-}\sigma\_ij \le \text{band}\_i \le \mu\_i + \sigma\_ij \text{ then band}\_i = 1, \text{ otherwise band}\_i = 0, \tag{5}$$

where μ and σ represent the mean and standard deviation of the grouped pixel samples (ROIs) from the sample data, respectively, i represents the band number of ALOS PALSAR, and j represents the positive real number of the selected standard deviation. The output was a binary image consisting of "mangrove" and "nonmangrove."

2.6 *Estimation of Aboveground Biomass*

The literature on estimation of the AGB of mangrove forests using PALSAR data is very small. Only a few studies[11,22–24] have established empirical relationships between L-band backscatter and the AGB of mangrove forests. The most significant difference between Takeuchi's and Hamdan's empirical relationships models is that Takeuchi's empirical relationships model uses conversion through general allometric height-biomass relations. We refer to this model as the indirect model. The empirical model is expressed as follows:[11]

$$\text{HH } (\sigma^\circ) = 3.6 \text{ ln } (\text{tree height}) - 23.7, \tag{6}$$

$$\text{HV } (\sigma^\circ) = 4.4 \text{ ln } (\text{tree height}) - 24.9, \tag{7}$$

$$\text{tree height} = 2.8 \text{ ln}(\text{DBH}) + 0.4, \tag{8}$$

$$\text{AGB} = 0.25\,\text{DBH}^{2.46}, \tag{9}$$

where DBH is the diameter at breast height and AGB is the aboveground biomass. In contrast, Hamdan et al.[23] directly related the backscatter value to the field biomass measurement, and thus we refer to it as the direct model. The empirical model is presented as follows:

$$\text{HH}\,(\sigma^\circ) = 0.472 \text{ ln}(\text{AGB}) - 12.326, \tag{10}$$

$$\text{HV}\,(\sigma^\circ) = 0.800 \text{ ln}(\text{AGB}) - 19.305. \tag{11}$$

3 Results and Discussion

3.1 *Backscattering Characteristics of Mangrove Forests in Southeast Asia*

We collected ALOS PALSAR data for the SEA region and determined the training samples as ROIs. Preprocessing was conducted by converting DN values to NRCS using Eqs. (1) and (2). In addition, the ROIs of 46 training samples were calculated to determine the backscattering characteristics of mangroves in the forms of mean and standard deviation values using Eqs. (3) and (4). The mean and standard deviations for each of the 46 ROIs can be seen in Fig. 2. Figure 2 shows the characterization of the backscattering coefficient of mangrove forests for the polarizations of HH and HV. The backscattering values of mangrove forests based on the HH polarization ranged from −10.88 to −6.65 dB, whereas the values based on the HV polarization were within the range −16.49 to −13.26 dB.[32]

Based on Fig. 2, each mangrove forest type has a wide range of backscattering values. The value depends on the physical and geometric conditions of the mangrove trees, as well as on environmental conditions such as weather dynamics, moisture, and the topography and altitude of tides.[33] The backscatter value also depends on a specific backscatter signal (e.g., radar calibration and orthorectification),[34,35] which is affected by the dielectric properties of the vegetation and ground surface.

3.2 *Spatial Distribution of Mangrove Forests Based on ALOS PALSAR*

We classified mangrove forests based on their backscattering characteristics and topography data. The classification was enhanced by visual interpretation using Landsat images and Google Earth imagery as reference data. In this case, the classification method used rule-based classification as defined by Eq. (5). We classified mangrove forests and nonmangrove forests on an area by area basis. The parameters used in the rule-based classification were HH, HV, and topography data. To determine the threshold value, the mean and standard deviation of the backscattering values of HH and HV were used. The threshold values of the backscattering on HH and HV can be seen in Table 2.

Using rule-based classification, we determined the spatial distribution of the mangrove forests in the SEA region (Fig. 3). The area of the mangrove forests in the SEA region was calculated as ∼5,098,834 ha with an overall accuracy of 82% (Table 3). The latter was done based on

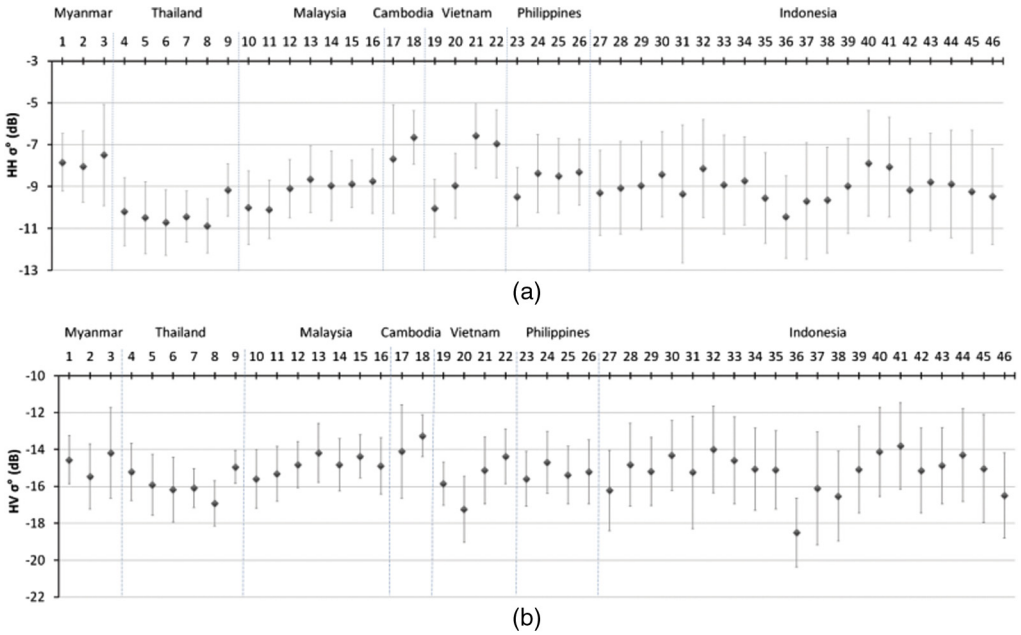

Fig. 2 Means and standard deviations of backscattering values of mangrove forests based on ALOS PALSAR polarization on (a) HH and (b) HV.

Table 2 Threshold values of mangrove forests for HH and HV.

	Threshold values of backscattering ALOS PALSAR 25-m resolutions (in dB)	
Area	HH	HV
Myanmar	−9.92 < mangrove < −5.07	−17.23 < mangrove < −11.72
Thailand	−12.29 < mangrove < −7.92	−18.14 < mangrove < −13.66
Malaysia	−11.76 < mangrove < −7.06	−17.20 < mangrove < −12.61
Cambodia	−10.28 < mangrove < −5.09	−16.64 < mangrove < −11.58
Vietnam	−10.50 < mangrove < −7.42	−19.03 < mangrove < −15.46
Philippines	−10.88 < mangrove < −6.50	−17.08 < mangrove < −13.02
Indonesia	−12.64 < mangrove < −5.37	−18.81 < mangrove < −11.47

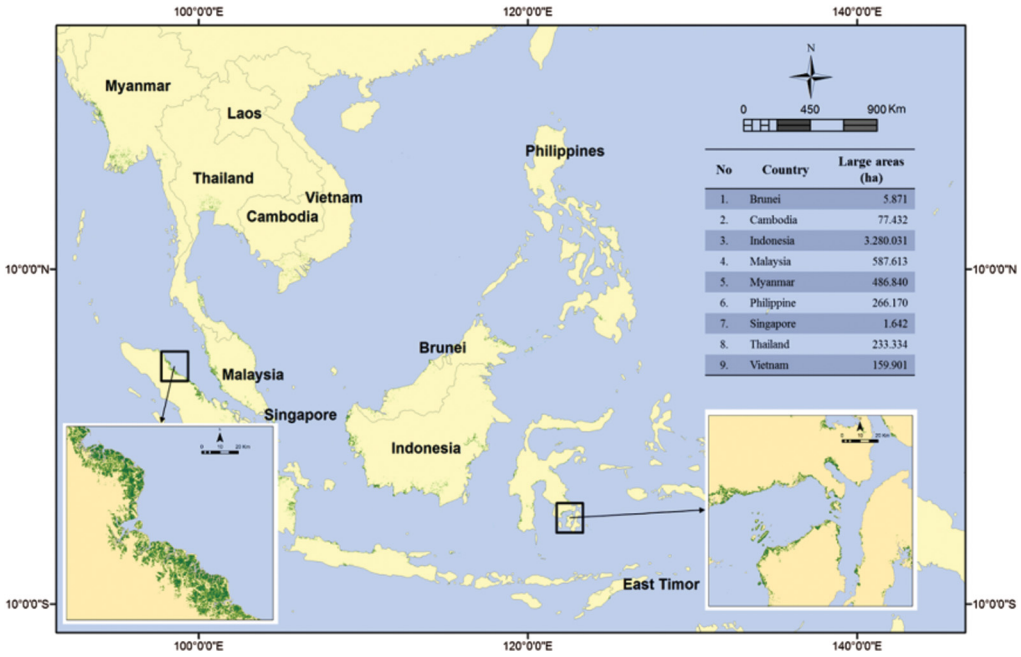

Fig. 3 Spatial distribution of mangrove forests in Southeast Asia.

Table 3 Overall accuracy.

		Reference data			
		Mangrove	Nonmangrove	Total	User's accuracy
Image classified	Mangrove	1,197,076	211,550	1,408,626	84.98%
	Nonmangrove	201,370	685,374	886,744	77.29%
	Total	1,398,446	896,924	2,295,370	
	Producer's accuracy	85.60%	76.41%		
			Overall accuracy = 82.01%		

Table 4 Sizes of mangrove forest areas in comparison with other studies.

No.	Area	Mangrove area (ha)	
		This study	Other studies
1.	Brunei	5871	17,100 in 1992[36]
2.	Cambodia	77,432	72,835 in 1997,[36] 83,600 in 2002[36]
3.	Indonesia	3,280,031	3,493,110 in 1988[36]
			3,244,018 in 2009[37]
4.	Malaysia	587,613	587,269 in 1995[36]
			564,606 in 2003[38]
5.	Myanmar	486,840	452,492 in 1996[36]
6.	Philippines	266,170	127,610 in 1990[36]
			256.185 in 2000[39]
7.	Thailand	233,334	244,085 in 2000[36]
			228.158 ha in 2007[40]
8.	Vietnam	159,901	252,500 in 1983[36]
			157,000 in 2005[41]

a confusion matrix, which takes advantage of ground truth derived from some reference data such as land use and land cover maps and visual interpretation from Landsat and Google Earth. The estimated areas of mangrove forests in each country in comparison with other studies are presented in Table 4. According to the table, there are differences in the large areas of mangrove forests determined by this study and the other studies. These differences arise from the different methods employed to estimate the large areas of mangrove forests; the other studies estimated the large areas of mangrove forests using data derived from a statistical log book, which is an old data version.

3.3 *Estimation of Aboveground Biomass of Mangrove Forests*

We applied two models to estimate the AGB of mangrove forests: the indirect model [Eqs. (6)–(9)] and the direct model [Eqs. (10) and (11)]. According to Sun et al.,[42] HV polarization of the RADAR data is the most sensitive for estimation of AGB. We estimated the average AGB of mangrove forests in the SEA region as 140.5 ± 136.1 Mg/ha. Some plots of the spatial distribution of the AGB of mangrove forests are presented in Fig. 4. However, on the low and flat topography, the backscatter value of mangrove forest is affected by tidal height. The deviation of backscatter value on the low and flat topography is around 1.6 dB for HV.[33] This study cannot identify information of tidal height because data are given from global 25-m resolution PALSAR and PALSAR-2 mosaics, so in this case, the AGB of mangrove forest that is estimated can be low or high.

Since the lack of ground measurement of the ABG of the mangrove forest on overall SEA still needs further research to validate our results, we have compared our results to those obtained by other studies (Table 5 and Fig. 5). We observed that the results based on the direct model are closer to those estimated by other studies than the indirect model. However, the direct model has a coefficient of determination (R^2) of 0.427 with a residual error of 61.32 Mg/ha.

According to Suzuki et al.,[48] one limitation of SAR in estimating AGB is that the backscatter intensity becomes saturated when the AGB volume exceeds a certain critical value. For example, estimation of the AGB of the mangrove forests in Matang Malaysia, where the AGB < 100 Mg/ha, gives the highest coefficient of determination (R^2) and the smallest root mean

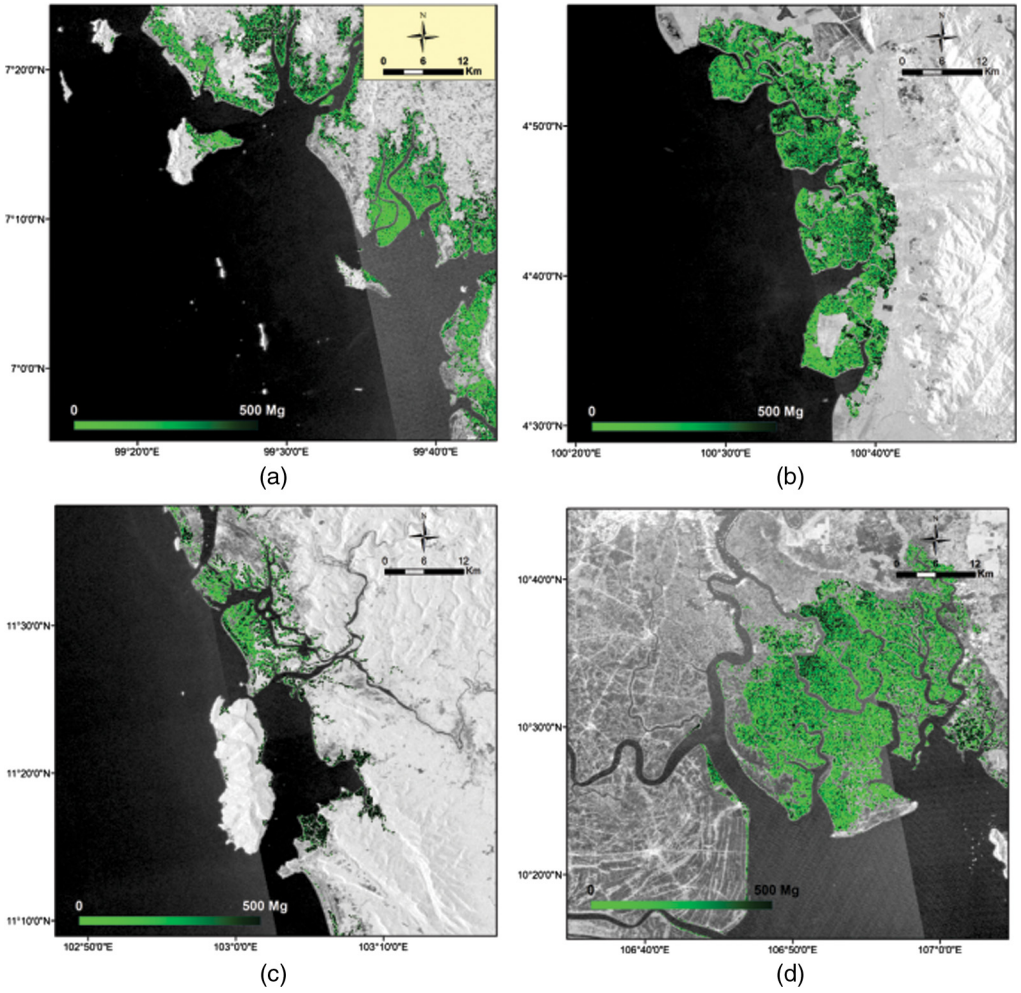

Fig. 4 Spatial distribution of the AGB of mangrove forests in the SEA region; (a) Suso Palian region, Thailand, (b) Jebong Perak region, Malaysia, (c) PeamKrasaop Wildlife Sanctuary, Cambodia, and (d) ThanhAn Can Gio, Vietnam.

square error (RMSE), whereas an AGB > 100 Mg/ha has a lower R^2 and a higher RMSE.[23] In addition, the saturation level of AGB for *Sonneratia caseolaris* and *Kandelia obovata* is above 100 Mg/ha.[23] According to Ghasemi et al.,[49] the saturation problem can be solved by applying an interferometry technique. However, this method has not been widely tested; thus, it is still not clear whether it can be used for AGB estimation of all types of mangrove forests.

We also have compared our result with Landsat data, where the actual optical images of the Landsat data with textural and spectral characteristics of the canopy and leaves are the main features used to distinguish among mangrove communities.[35,50] According to Fig. 6 the results of the classification of mangroves and nonmangroves on ALOS PALSAR imagery are almost the same as those produced by Landsat imagery. However, in this study, not only can be classified mangrove and non-mangrove, but also we have estimated above ground biomass of mangrove forest.

4 Conclusions

In this study, an AGB dataset of mangrove forests in SEA was developed. The spatial distribution of the mangrove forests in SEA was found to be 5.1 million ha with an overall accuracy of 82%. The estimated average AGB of the mangrove forests in SEA was found to be 140.5 ± 136.1 Mg/ha. The direct model was also determined to be more accurate for estimation of the AGB of mangrove forests than the indirect model. However, saturation in estimating AGB needs

Table 5 Comparison of AGB estimation of mangrove forests using the indirect and direct models with other studies.

No.	Location	Major species	Indirect model (Mg/ha)	Direct model (Mg/ha)	Other studies (Mg/ha)
1.	Perak, Malaysia	*Rhizophora apiculata*	250.5	101.72	99.4[23]
2.	Aceh, Indonesia	—	96.5	46.8	11.68[43]
3.	Chumpon, Thailand	*Rhizophora apiculata*	807.4	231.4	216[6]
4.	Pang-nga, Thailand	Mix	494.1	166.3	108[44]
5.	Kuala Selangor, Malaysia	*Bruguiera parviflora*	411.33	146.3	144.47[45]
6.	MuiCamau, Vietnam	*Avicennia alba* *Rhizophora apiculata*	167.2	74.2	$90.2 + 15.8$[46]
7.	West Kalimantan, Indonesia	*Avicennia marina* *Rhizophora apiculata* *Rhizophora stylosa* *Rhizophora alba* *Rhizophora mucronata* *Bruguiera gymnorrhiza* *Xylocarpus granatum*	467.1	159.9	$159.1 + 69.5$[5]
8.	Papua, Indonesia	*Avicennia marina* *Rhizophora apiculata* *Rhizophora stylosa* *Rhizophora alba* *Rhizophora mucronata* *Bruguiera gymnorrhiza* *Xylocarpus granatum*	924.3	252.56	$213.8 + 129.8$[5]
9.	The Philippines	*Avicennia officinalis*	1.342	319.3	297.2[47]

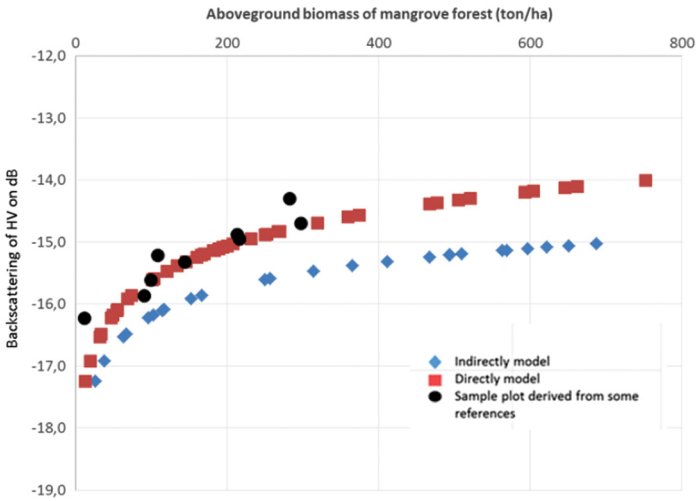

Fig. 5 Comparison of AGB derived from backscattering of HV on ALOS PALSAR.

to be reduced by integrating multisource data, including different wavelengths for optical data and microwaves. Thus, in future studies, development of more appropriate procedures and approaches is still required to reduce uncertainty and also the conducting and collecting of field survey measurements is required for validation.

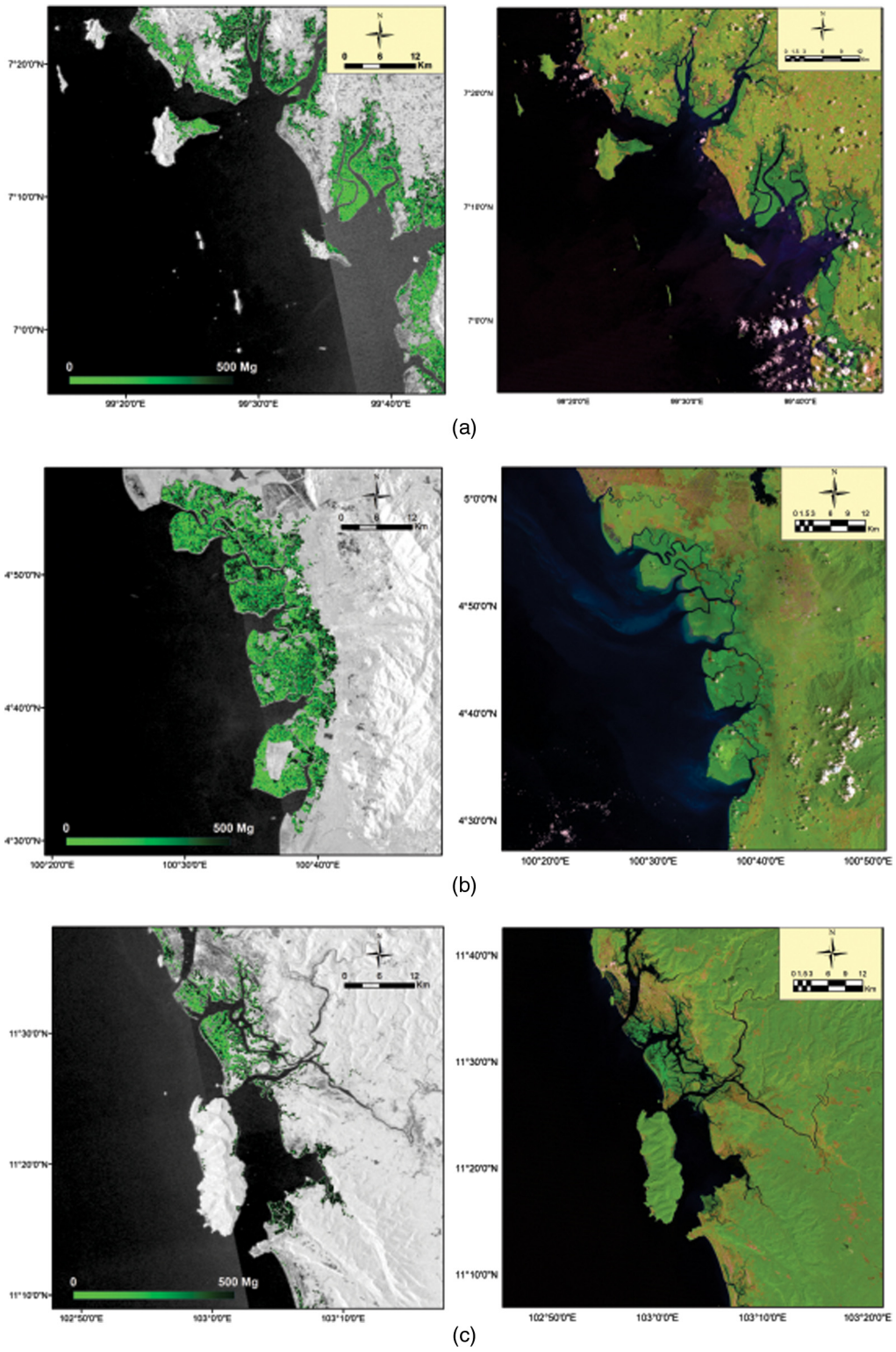

Fig. 6 Comparison of AGB estimated based on ALOS PALSAR and Landsat imagery data in (a) Suso Palian region, Thailand, (b) Jebong Perak region, Malaysia, and (c) Peam Krasaop Wildlife Sanctuary, Cambodia.

Acknowledgments

The authors would like to thank the Ministry of Research, Technology, and Higher Education of the Republic of Indonesia (RISTEKDIKTI) for all their support. Also the authors would like

to thank LPPM-ITENAS, JAXA-JAPAN, and Anggun Tridawati from Lampung University for their support.

References

1. M. N. Suratman, "Carbon sequestration potential of mangroves in Southeast Asia," in *Managing Forest Ecosystems: The Challenge of Climate Change*, F. Brafo et al., Eds., Vol. 1, pp. 297–315, Springer, New York (2008).
2. W. Giesen et al., *Mangrove Guidebook for Southeast Asia*, Wetlands International, Bangkok (2007).
3. C. Nellemann, *Blue Carbon, A Rapid Response Assessment*, 80 pp., United Nations Environment Programme, Norway (2009).
4. D. C. Donato et al., "Mangroves among the most carbon-rich forests in the tropics," *Nat. Geosci.* **4**(5), 293–297 (2011).
5. D. Murdiyarso et al., "The potential of Indonesian mangrove forests for global climate change mitigation," *Nat. Clim. Change* **5**, 1089–1092 (2015).
6. D. M. Alongi and P. Dixon, "Mangrove primary production and above and below-ground biomass in Sawi Bay, Southern Thailand," *Phuket Mar. Biol. Center Spec. Publ.* **22**, 31–38 (2000).
7. R. A. Houghton et al., "Importance of biomass in the global carbon cycle," *J. Geophys. Res. Biogeosci.* **114**, G00E3 (2009).
8. W. Giesen and S. Wulffraat, "Indonesian mangroves part I: plant diversity and vegetation," *Trop. Biodivers.* **5** (2), 11–23 (1998).
9. R. Tabuchi and S. B. Unyavejchewin, "Development of mangrove stands in Southeast Asia: with special reference to the west coast of the Malay Peninsula," *Global Environ. Res.* 215–221 (2013).
10. C. Giri et al., "Status and distribution of mangrove forests of the world using earth observation satellite data," *Glob. Ecol. Biogeogr.* **20**(1), 154–159 (2011).
11. W. Takeuchi et al., "Above ground biomass mapping of mangrove forest in Vietnam by ALOS PALSAR," in *3rd Int. Asia-Pac. Conf. Synth. Aperture Radar (APSAR)*, Seoul, pp. 1–3 (2011).
12. A. Aslan et al., "Remote sensing of environment mapping spatial distribution and biomass of coastal wetland vegetation in Indonesian Papua by combining active and passive remotely sensed data," *Remote Sens. Environ.* **183**, 65–81 (2016).
13. A. Held et al., High resolution mapping of tropical mangrove ecosystems using hyperspectral and radar remote sensing, *Int. J. Remote Sens.* **24**(13), 2739–2759 (2003).
14. T. Häme et al., "Improved mapping of tropical forests with optical and SAR imagery, part II: above ground biomass estimation," *IEEE J. Sel. Top. Appl. Earth Obs. Remote Sens.* **6**(1), 92–101 (2013).
15. F. M. Henderson and A. J. Lewis, "Radar detection of wetland ecosystems: a review," *Int. J. Remote Sens.* **29**(20), 5809–5835 (2008).
16. N. M. Yusoff et al., "Phenology and classification of abandoned agricultural land based on ALOS-1 and 2 PALSAR multi-temporal measurements," *Int. J. Digital Earth* **10**(2), 155–174 (2017).
17. S. Darmawan et al., "An investigation of age and yield of fresh fruit bunches of oil palm based on ALOS PALSAR 2," *IOP Conf. Series: Earth Environ. Sci.* **37**, 012037 (2016).
18. S. Sinha et al., "A review of radar remote sensing for biomass estimation," *Int. J. Environ. Sci. Technol.* **12**(5), 1779–1792 (2015).
19. E. T. A. Mitchard et al., "Using satellite radar backscatter to predict above-ground woody biomass: a consistent relationship across four different African landscapes," *Geophys. Res. Lett.* **36**(23), 1–6 (2009).
20. T. Le Toan et al., "The BIOMASS mission: mapping global forest biomass to better understand the terrestrial carbon cycle," *Remote Sens. Environ.* **115**(11), 2850–2860 (2011).
21. Y. Yu and S. Saatchi, "Sensitivity of L-band SAR backscatter to aboveground biomass of global forests," *Remote Sens.* **8**(6), 522 (2016).

22. A. C. Morel et al., "Estimating aboveground biomass in forest and oil palm plantation in Sabah, Malaysian Borneo using ALOS PALSAR data," *For. Ecol. Manage.* **262**(9), 1786–1798 (2011).
23. O. Hamdan, H. Khali Aziz, and I. MohdHasmadi, "L-band ALOS PALSAR for biomass estimation of Matang Mangroves, Malaysia," *Remote Sens. Environ.* **155**, 69–78 (2014).
24. P. Tien Dat, Y. Kunihiko, and B. DieuTien, "Biomass estimation of *Sonneratia caseolaris* (l.) Engler at a coastal area of Hai Phong city (Vietnam) using ALOS-2 PALSAR imagery and GIS-based multi-layer perceptron neural networks," *GISci. Remote Sens.* **54**, 329–353 (2016).
25. P. Tien Dat and Y. Kunihiko, "Aboveground biomass estimation of mangrove species using ALOS-2 PALSAR imagery in Hai Phong city, Vietnam," *J. Appl. Remote Sens.* **11**(2), 026010 (2017).
26. V. Sasan et al., "Improving accuracy estimation of forest aboveground biomass based on incorporation of ALOS-2 PALSAR-2 and sentinel-2A imagery and machine learning: a case study of the Hyrcanian Forest Area (Iran)," *Remote Sens.* **10**, 172 (2018).
27. R. Lucas et al., "Characterisation and monitoring of Mangroves using ALOS PALSAR data," Eorc. Jaxa. Jp., 2009, http://www.eorc.jaxa.jp/ALOS/en/kyoto/phase_1/KC-Phase1-report_Lucas_WT.pdf (accessed 14 April 2015).
28. T. Nathan et al., "Distribution and drivers of global mangrove forest change, 1996 ± 2010," *PLoS One* **12**(6), e0179302 (2017).
29. B. Pete et al., "The global mangrove watch: a new 2010 global baseline of mangrove extent," *Remote Sens.* **10**, 1669 (2018).
30. P. Tien Dat et al., "Remote sensing approaches for monitoring mangrove species, structure, and biomass: opportunities and challenges," *Remote Sens.* **11**, 230 (2019).
31. M. Shimada et al., "PALSAR radiometric and geometric calibration," *IEEE Trans. Geosci. Remote Sens.* **47** (12), 3915–3932 (2009).
32. S. Darmawan et al., "Characterization and spatial distribution of mangrove forest types based on ALOS-PALSAR mosaic 25-m resolution in Southeast Asia," *IOP Conf. Ser.: Earth Environ. Sci.* **37**, 012035 (2016).
33. S. Darmawan et al., "Impact of topography and tidal height on ALOS PALSAR polarimetric measurements to estimate aboveground biomass of mangrove forest in Indonesia," *J. Sens.* **2015**, 1–13 (2015).
34. J. J. Van Zyl, "The effect of topography on radar scattering from vegetated areas," *Int. Geosci. Remote Sens. Symp.* **2**(1), 1132–1134 (1992).
35. C. Kuenzer et al., "Remote sensing of mangrove ecosystems: a review," *Remote Sens.* **3**, 878–928 (2013).
36. FAO, "Status and trends in mangrove area extent worldwide,"M. L. Wilkie and S. Fortuna," Forest Resources Assessment Working Paper No. 63, Forest Resources Division, FAO, Rome (2003).
37. C. Kusmana, "Distribution and current status of mangrove forests in Indonesia," in *Mangrove Ecosystems of Asia: Status, Challenges and Management Strategies*, I. Faridah-Hanum et al., Eds., Vol. **1**, pp. 38–59, Springer, New York (2013).
38. A. Latiff and I. Farida-Hanum, "Mangrove ecosystem of Malaysia: status, challenges and management strategies," in *Mangrove Ecosystems of Asia; Status, Challenges and Management Strategies*, I. Faridah-Hanum, Eds., Vol. **1**, pp. 1–18, Springer, New York (2013).
39. J. B. Long and C. Giri, "Mapping the Philippines' mangrove forests using Landsat imagery," *Sensors* **11**(3), 2972–2981 (2011).
40. N. Pumijumnong, "Mangrove forests in Thailand," in *Mangrove Ecosystems of Asia: Status, Challenges and Management Strategies*, I. Faridah-Hanum et al., Eds., Vol. 1, pp. 62–77, Springer, New York (2013).
41. R. Mcnally, A. McEwin, and T. Holland, "The potential for mangrove carbon projects in Vietnam," Connecting People's Capacity, Netherlands Development Organization March, 44 (2011).
42. G. Sun, K. J. Ranson, and V. I. Kharuk, "Radiometric slope correction for forest biomass estimation from SAR data in the Western Sayani Mountains, Siberia," *Remote Sens. Environ.* **79**(2–3), 279–287 (2002).

43. D. M. Yuwono, *Pemetaan Mangrove Sumatera, Provinsi Aceh, Sumatera Utara dan Riau*, Badan Infromasi Geospasial (BIG), Bogor (2013).
44. P. Phongsuksawat, "Determination of tree biomass in the mangrove habitat study area, Changwat Phangna," Master's Thesis, Kasetsart University, Thailand (2002).
45. M. Hossain et al., "Net primary productivity of *Bruguiera parviflora* (Wight & Arn.) dominated mangrove forest at Kuala Selangor, Malaysia," *For. Ecol. Manage.* **255**(1), 179–182 (2008).
46. N. T. Tue et al., "Carbon storage of a tropical mangrove forest in MuiCa Mau National Park, Vietnam," *Catena* **121**, 119–126 (2014).
47. A. C. Abino, J. A. A. Castillo, and Y. J. Lee, "Assessment of species diversity, biomass and carbon sequestration potential of a natural mangrove stand in Samar, the Philippines," *For. Sci. Technol.* **10**(1), 2–8 (2014).
48. R. Suzuki, Y. Kim, and R. Ishii, "Sensitivity of the backscatter intensity of ALOS/PALSAR to the above-ground biomass and other biophysical parameters of boreal forest in Alaska," *Polar Sci.* **7**(2), 100–112 (2013).
49. N. Ghasemi, M. R. Sahebi, and A. Mohammadzadeh, "A review on biomass estimation methods using synthetic aperture radar," *Int. J. Geomatics Geosci.* **1**(4), 776–788 (2011).
50. G. Winarso et al., "Mangrove above ground biomass estimation using combination of Landsat 8 and ALOS PALSAR data," *Int. J. Remote Sens. Earth Sci.* **12**(2), 85–96 (2015).

Biographies of the authors are not available.